Influence of piston slow shot speed variation in shot sleeve on melt flow, solidification and defects formation in HPDC process: a numerical modelling study

KUN DOU[1*], EWAN LORDAN[1], YIJIE ZHANG[1]
Brunel Centre for Advanced Solidification Technology (BCAST)
Brunel University London
Kingston Lane, Uxbridge, Middlesex, London, UB8 3PH
UNITED KINGDOM
Kun.Dou@brunel.ac.uk

Abstract: - In this paper, the high pressure die casting (HPDC) process for Al-Si alloy is modelled with finite element method in ProCAST platform. The shot sleeve filling and die filling processes are described based on actual process parameters from HPDC machine. Three sets of piston slow shot curves are used to study its influence on free surface evolution and defects formation in final casting. According to final distribution uniformness of entrained air and oxides, the optimum piston slow shot profile is determined and can be further transferred into process control of actual HPDC process.

Key-Words: - HPDC, Shot Sleeve, Fluid Flow, CFD, Air Entrainment, Oxides

1 Introduction

During the high pressure die casting process, the quality and mechanical properties of the casting is dependent on the microstructure formation during the melt filling and subsequent solidification process[1–5]. Due to the contact and mixing of melt with air during shot sleeve pre-filling subsequent injection in die cavity, defects such as gas pores, oxides would occur and inherent randomly in final casting, which would deteriorate the mechanical properties of the casting and cause variability in different positions[6–9]. The melt flow in shot chamber forced by plunger movement is a complex process combining fluid flow, heat transfer and solidification. In conventional cold chamber HPDC process, the melt height gradually accumulates and fills the chamber space during the 1st stage plunger movement, driving the residual air out through the pouring hole and vent in die region. Then, in the 2nd stage plunger movement, plunger acceleration would force the melt flow into the die cavity through a narrow ingate causing turbulence flow[10–12].

Here in this paper, the characteristics of melt flow in shot chamber are studied using numerical modelling approach. Variation of plunger slow shot speed is considered and wave formation, air entrainment as well as oxides formation probability for melt in shot chamber and final casting are calculated using software package ProCAST.

2 Model Establishment

The entire HPDC machine model is established through CAD method first. Then, the CAD model is imported into Visual-Mesh module in ProCAST software for mesh generation. The CAD model and finite element model are shown in **Figure 1**.

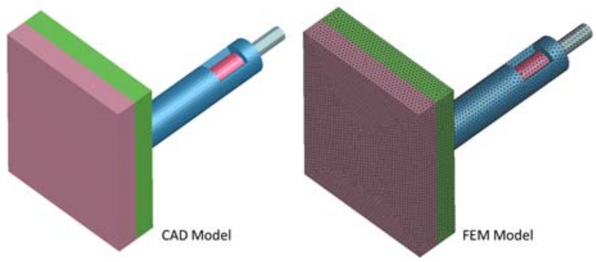

Figure 1 CAD and FEM models of HPDC machine

2.1 Governing Equations

Based on finite element method, a three-dimensional mathematical model for HPDC process is established to calculate the melt flow, heat transfer and solidification. General governing equations used are listed below. Typical defects are described using corresponding models, which will be described later.

Continuous Equation

$$\nabla \cdot \vec{\boldsymbol{v}} = 0 \quad (1)$$

Momentum Equation

$$\frac{\partial(\rho\vec{v})}{\partial t} + \nabla \cdot (\rho\vec{\boldsymbol{v}} \cdot \boldsymbol{v_i}) = \nabla \cdot (\mu\, \nabla\vec{\boldsymbol{v}}) - \nabla p \quad (2)$$

To describe the turbulence of melt during injection process, $\mathrm{k}-\varepsilon$ turbulence model is used.

$$\frac{\partial(\rho k)}{\partial t} + \nabla \cdot (\rho \vec{\boldsymbol{v}} k) = \nabla \cdot \left[\left(\mu + \frac{\mu_t}{\sigma_k} \right) \nabla k \right] + G_k - \rho \varepsilon$$

(3)

$$\frac{\partial(\rho \varepsilon)}{\partial t} + \nabla \cdot (\rho \vec{\boldsymbol{v}} \varepsilon) = \nabla \cdot \left[\left(\mu + \frac{\mu_t}{\sigma_\varepsilon} \right) \nabla \varepsilon \right] + \frac{\varepsilon}{k} \left(C_{1\varepsilon} G_k - C_{2\varepsilon} \frac{\varepsilon^2}{k} \right) \quad (4)$$

Energy Equation:

$$\frac{\partial(\rho c_p T)}{\partial t} + \nabla \cdot (\rho \vec{\boldsymbol{u}} T) = \nabla \cdot (k \, \nabla T) + S_T \quad (5)$$

The solidification source term S_T of the melt is described using enthalpy method as follows:

$$\mathrm{H(T)} = \int_0^T C_P(T) dT + L(1 - f_s) \quad (6)$$

In above equations, $\boldsymbol{v}$ is velocity, ρ is time, P is pressure, μ is melt viscosity, k and ε are turbulence parameters, T is temperature, c_p is specific heat, L is latent heat during solidification, H is enthalpy.

2.2 Boundary Condition

The boundary condition used in the model are listed in Table 1.

Table 1 Initial/boundary conditions used in subsequent modelling

Alloy type	A380	Sleeve temperature	180□
Liquidus	594□	Sleeve length	480mm
Solidus	513□	Die/sleeve material	H13 steel
Pouring temperature	670□	Die surface temperature	150□

Thermophysical parameters of A380 alloy are calculated based on chemical compositions and database[13,14] from ProCAST software, which are shown in **Figure 2**.

The solid fraction curve is calculated based on Scheil micro-segregation model, which corresponds to no diffusion of solute elements in the solid and complete mixing in the liquid, which is reasonable considering the high cooling rate during the HPDC process. The enthalpy, density, thermal conductivity and viscosity are treated as temperature-dependent, which considers the influence of phase change during alloy solidification process.

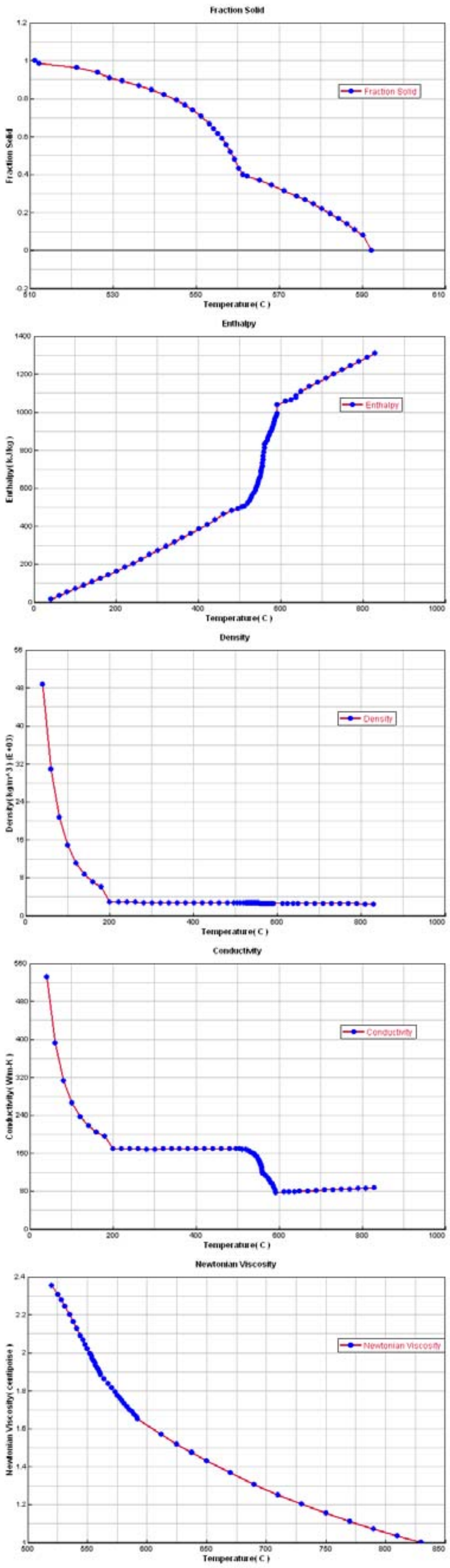

Figure 2 Thermophysical parameters of A380 alloy

The piston velocity profiles are set as in **Figure 3**, it could be seen that it mainly consists of slow shot stage and fast injection stage. In this work, three sets of slow shot velocity (0.2-0.3m/s, .4-0.6m/s and 0.6-1m/s) are selected for study.

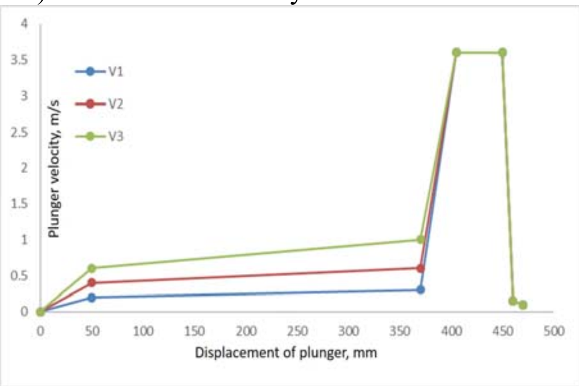

Figure 3 Piston velocity profiles used in this work

2.3 Defects Prediction Model

Volume of Fluid (VOF) method is used to describe the evolution of melt free surface. The air entrainment amount in the melt and final casting is predicted qualitatively using GAS model in ProCAST software. If non-zero value is given for GAS, the unfilled casting regions are assumed to be filled with ideal gas. Such a region can be (1) “widely open”, i.e. connected to a pressure BC which has a value of PREF. (2) “trapped” (including regions with vents). GAS calculation is for the trapped regions, depending on the GAS parameter, the trapped gas amount and gas properties are calculated. Two important parameters are defined in GAS model, PREF and TGAS. For GAS model, a portion of gas will be trapped, the portion increase linearly from 0 to 10% depending on (P-PREF) up to 100 * PREF, it is capped at 10%, 100 * PREF.

For oxides prediction, the oxides indicator in ProCAST software is used. The fluid front tracking indicator "Free surface time exposure" has the units of [cm^2*s]. The principle of calculation of this indicator is the following:

At each point of the free surface, the free surface area multiplied by the time. This value is cumulated with the value of the previous timestep. In addition, this value is transported with the free surface and with the fluid flow. When two free surfaces are meeting, both values are added. When there is no free surface at a given location, the value of the front tracking indicator can still be transported by the fluid movement. This indicator allows to identify the amount of oxides formed at the free surface and where they are most likely to end-up as well as to study the flow junctions.

Based on above model, the air entrainment during HPDC process are qualitatively assessed with variation of slow shot speed during injection in shot sleeve.

3 Results

The HPDC process of tensile test samples made of A380 alloy has been simulated. As shown in **Figure 4**, during the first stage of injection, when the piston moves at slow speed, a shallow wave is formed at the free surface of the melt. During the second stage, the piston velocity increases and the melt is injected into the die at high speed. The simulation predicts the evolution of different physical quantities such as the melt velocity, temperature, and solid fractions. In addition, it brings insight about the distribution of defects. The colour maps represent the amounts of entrapped air.

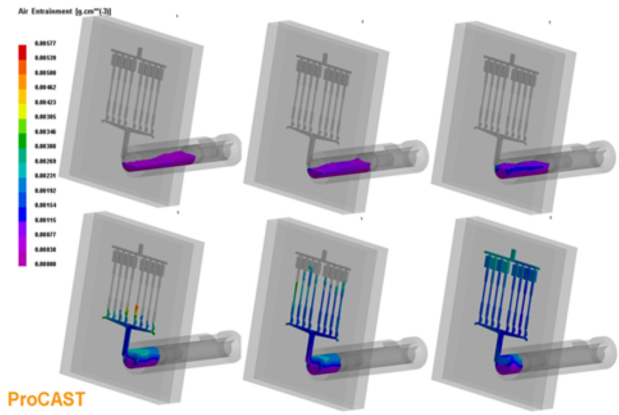

Figure 4 Simulation of flow and air entrainment during high pressure die casting of A380 test samples

The porosities formed in HPDC casting process are simulated based on flow, solidification and gas segregation, as is shown in **Figure 5**. Further optical micrography observations are performed to validate the prediction, which shows correspondence.

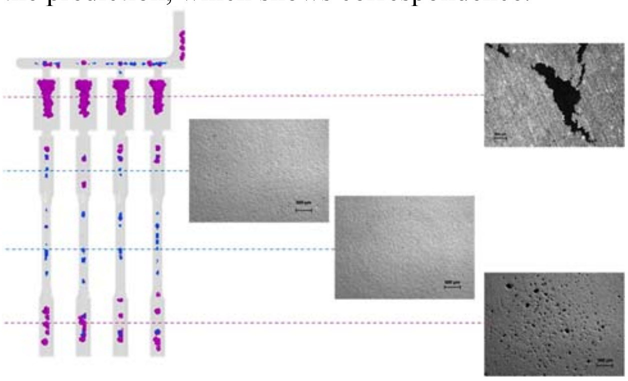

Figure 5 Comparison of porosity simulation against observation

4 Discussions

Motion of melt flow in shot sleeve at different slow shot speed are modelled, the velocity magnitude profiles are shown in Fig.1, evolution of the free surface and air entrainment amount are shown in **Figure 6** (a)-(c).

From **Figure 6** (a), it is clearly seen that during the slow shot phase of 0.2-0.3m/s, the melt flow is activated with motion of plunger and the free surface is relatively calm, there is little air entrainment in the filling and injection process. By increasing the plunger velocity to 0.4-0.6m/s, it could be seen from **Figure 6** (b) that the wave is formed at the free surface front and there is little air entrainment. As a further step to analyze the melt flow, plunger velocity is increased to 0.6-1m/s and the filling sequence is shown in **Figure 6** (c). It could be observed that as plunger accelerates, melt free surface would accumulate and contact with top of the chamber and collapse afterwards.

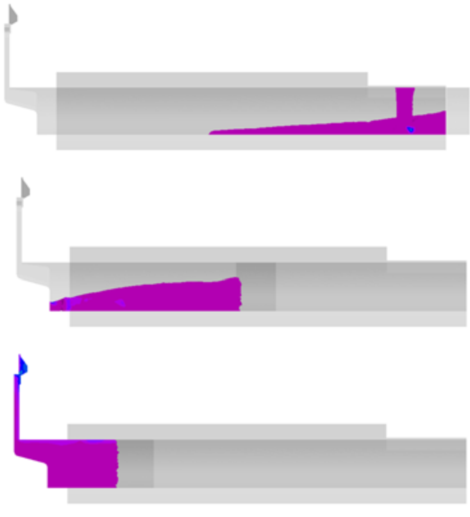

(a) filling of shot sleeve at slow stage velocity of 0.2-0.3m/s

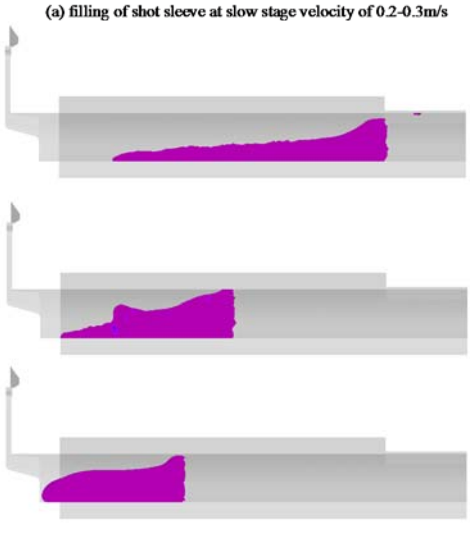

(b) filling of shot sleeve at slow stage velocity of 0.4-0.6m/s

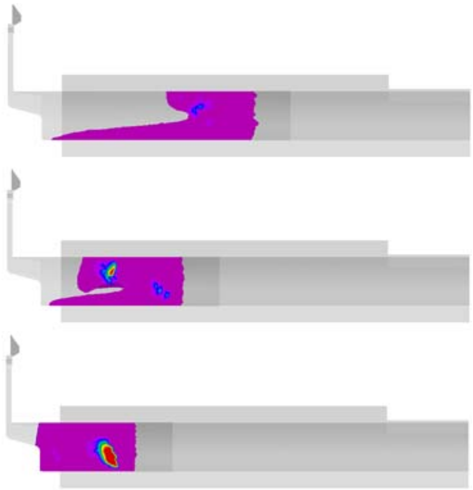

(c) filling of shot sleeve at slow stage velocity of 0.6-1m/s

Figure 6 Evolution of melt filling process inside shot sleeve at different slow shot velocity (contour area represents air entrainment amount)

During this process, a portion of air is captured at the fluid front, which would be transported into die cavity and reside in final casting. From comparison of **Figure 6** (a)-(c), it could be concluded that for minimizing air entrainment, the plunger velocity during slow shot stage should not exceeds 0.6m/s. **Figure 7** compares the air entrainment distribution in the actual casting volume produced at different slow injection speed. While **Figure 8** compares the oxide distribution in the castings correspondingly.

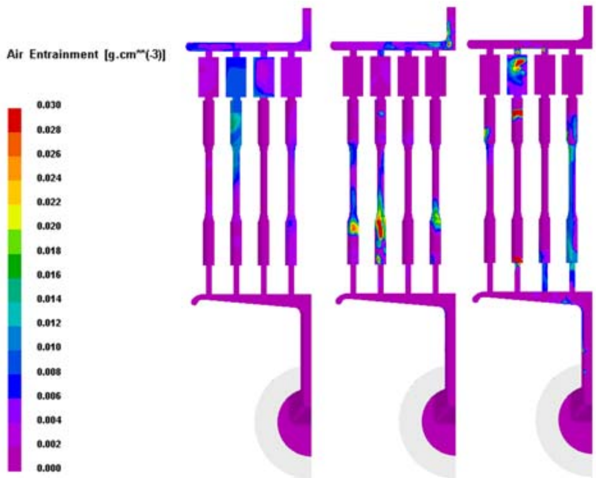

Figure 7 Air entrainment distribution in casting volume produced at various slow shot velocity in half symmetry (from left to right: 0.2-0.3m/s, 0.4-0.6m/s, 0.6-1m/s)

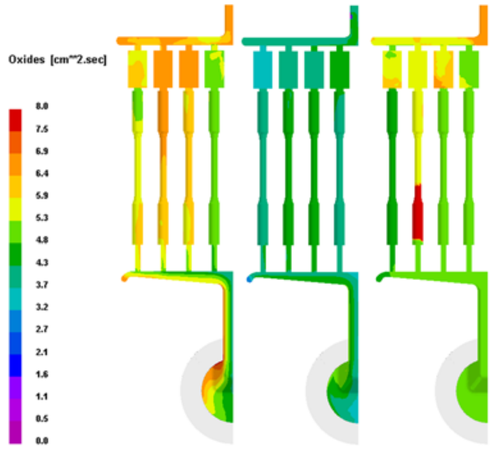

Figure 8 Oxides distribution in casting volume produced at various slow shot velocity in half symmetry (from left to right: 0.2-0.3m/s, 0.4-0.6m/s, 0.6-1m/s)

It could be seen that casting produced with shot slow speed of 0.2-0.3m/s exhibit lowest level of air entrainment and when slow shot speed exceeds 0.6m/s, air entrainment amount in casting would increase and distribute unevenly. Regarding oxides formation and distribution, the optimal slow shot speed is 0.4-0.6m/s, under which the oxides tendency at different casting locations are relatively uniform and oxides amount tend to be low compared with others condition.

As the mechanical properties of the casting is a comprehensive result of casting microstructure and its interaction with defects. Obtaining a uniform microstructure with less defects is the final goal to improve mechanical properties and achieve property stability. For the study in this paper, the increased slow stage velocity of 0.4-0.6m/s could reduce and uniformize oxides formation without introducing too much air in the melt, in the meantime, it could limit the formation of externally solidified crystals (ESCs) by reducing the heat loss of the melt in shot sleeve.

5 Conclusion

In this paper, a finite element model for high pressure die casting process of A380 alloy is established and fluid flow, solidification and defects formation are studied numerically. On this basis, influence of piston slow shot profiles is analyzed. In order to decrease the formation and uniformize the distribution of air and oxides, an optimum piston slow shot velocity is determined, which can be further used in actual HPDC process, through which to improve the mechanical properties of the as-cast products.

Acknowledgements: This project is financially supported by EPSRC UK in the EPSRC Centre for Innovative Manufacturing in Liquid Metal Engineering (The EPSRC Centre—LiME).

References:

[1] S. Tzamtzis, H. Zhang, M. Xia, N.H. Babu, Z. Fan, Recycling of high grade die casting AM series magnesium scrap with the melt conditioned high pressure die casting (MC-HPDC) process, Mater. Sci. Eng. A. 528 (2011) 2664–2669. doi:10.1016/j.msea.2010.12.001.

[2] X. Zhu, P. Blake, K. Dou, S. Ji, Strengthening die-cast Al-Mg and Al-Mg-Mn alloys with Fe as a beneficial element, Mater. Sci. Eng. A. 732 (2018) 240–250. doi:10.1016/j.msea.2018.07.005.

[3] M. Xia, S. Mitra, D. Brij, G. Liu, Z. Fan, Melt-conditioned, high-pressure die casting of Mg-Zn-Y Alloy, Metall. Mater. Trans. B Process Metall. Mater. Process. Sci. 41 (2010) 209–213. doi:10.1007/s11663-009-9312-5.

[4] S. Otarawanna, C.M. Gourlay, H.I. Laukli, A.K. Dahle, Formation of the surface layer in hypoeutectic Al-alloy high-pressure die castings, Mater. Chem. Phys. 130 (2011) 251–258. doi:10.1016/j.matchemphys.2011.06.035.

[5] S. Ji, F. Yan, Z. Fan, A High Strength Aluminium Alloy for High Pressure Die Casting, Light Met. 2016. (2016) 207–210. doi:10.1002/9781119274780.ch35.

[6] R. Zamora, F. Faura, J. López, J. Hernández, Experimental verification of numerical predictions for the optimum plunger speed in the slow phase of a high-pressure die casting machine, Int. J. Adv. Manuf. Technol. 33 (2007) 266–276. doi:10.1007/s00170-006-0456-z.

[7] S. Li, S. Xiong, B. Liu, M. Li, J. Allison, Numerical simulation of flow-induced air entrapment defects in the high pressure die casting process, (2010).

[8] D. Dispinar, J. Campbell, The use of bifilm index as an assessment of liquid metal quality, TMS Annu. Meet. 0461 (2005) 23–30. doi:10.1179/136404606225023300.

[9] R.K. Tiwari, T.R. Chauhan, Flow pattern analysis of melted aluminum in shot sleeve of pressure dies casting and minimizing the defect, 3 (2015) 161–180.

[10] S.M. Hosseini, Z. Utlu, Design optimization of clutch housing mold by fluid flow and

solidification simulation, J. Mech. Sci. Technol. 30 (2016) 2731–2742. doi:10.1007/s12206-016-0535-5.

[11] H.I. Laukli, O. Lohne, S. Sannes, H. Gjestland, L. Arnberg, Grain size distribution in a complex AM60 magnesium alloy die casting, Int. J. Cast Met. Res. 16 (2003) 515–521. doi:10.1080/13640461.2003.11819629.

[12] W. Yu, Y. Cao, X. Li, Z. Guo, S. Xiong, Determination of Interfacial Heat Transfer Behavior at the Metal / Shot Sleeve of High Pressure Die Casting Process of AZ91D Alloy, 33 (2017) 52–58.

[13] J. Guo, C. Beckermann, K. Carlson, D. Hirvo, K. Bell, T. Moreland, J. Gu, J. Clews, S. Scott, G. Couturier, D. Backman, Microporosity prediction and validation for Ni-based superalloy castings, IOP Conf. Ser. Mater. Sci. Eng. 84 (2015) 1–7. doi:10.1088/1757-899X/84/1/012003.

[14] J. Guo, M. Samonds, Modeling of alloy casting solidification, Jom. 63 (2011) 19–28. doi:10.1007/s11837-011-0104-4.